20th International Young Scientist Conference **"Developments in Optics and Communications 2024"**

ABSTRACT BOOK

Optical Materials and Phenomena

Laser Physics and Spectroscopy

Communications

Biophotonics

Vision Science

DEVELOPMENTS in Optics and Communications 2024

May 2-3

WWW.DOCRIGA.LV

SPIE. STUDENT CHAPTER UNIVERSITY OF LATVIA

UNIVERSITY OF LATVIA

82nd International Scientific Conference of the University of Latvia 2024

UNIVERSITY OF LATVIA INSTITUTE OF ATOMIC PHYSICS AND SPECTROSCOPY

DOC 2024 Abstract Book

20th International Young Scientist conference

Developments in Optics and Communications 2024

Editor: Inga Brice
Institute of Atomic Physics and Spectroscopy
University of Latvia
Jelgavas street 3, Riga, LV1004, Latvia

ISBN xxxx

Cover design: Inga Brice

www.docriga.lv

Welcome

Dear participants of **DOC 2024**,

The Organizing Committee kindly welcomes you to the 20th International Young Scientist conference "Developments in Optics and Communications 2024". The purpose of this conference is to bring together students and young scientists to discuss latest scientific results and upcoming trends in the fields of optics and photonics.

"*Every brilliant experiment, like every great work of art, starts with an act of imagination.*" – Jonah Lehrer

Imagination is important to more than just creativity and arts which are considered almost an opposite of science. After all artists use imagination to construct new make belief fantastic worlds and characters. Things that are not real. However, in science imagination is also important. It is the foundation of every new theory and every new experiment our minds conjure that eventually lead to new discoveries, advancing technologies, and knowledge.

The Organizing Committee sincerely hopes that you will enjoy this conference and get new ideas and collaborations for your future in research

Best regards,
DOC 2024 Organizers

The Organizing Committee

DOC chair

Lase Milgrave
PhD student, scientific assistant
University of Latvia

Organizers

- Zane Jansone-Langina
- Kristine Kalnica Dorosenko
- Kristians Draguns
- Inga Brice
- Ilze Oshina
- Madara Leimane

Scientific committee

- Prof. Ruvin Ferber
  Faculty of Physics and Mathematics, University of Latvia
- Prof. Māris Ozoliņš
  Department of Optometry and Vision science, University of Latvia
- Prof. Uldis Rogulis
  Institute of Solid State Physics, University of Latvia
- Prof. Janis Spigulis
  Institute of Atomic Physics and Spectroscopy, University of Latvia

Contents

Invited Speakers

Talks

Optical Materials and Phenomena

Part I
Invited Speakers

SPIE. STUDENT CHAPTER UNIVERSITY OF LATVIA

UNIVERSITY OF LATVIA

82nd International Scientific Conference of the University of Latvia 2024

UNIVERSITY OF LATVIA
INSTITUTE OF ATOMIC PHYSICS AND SPECTROSCOPY

Quantum light sources: from novel materials to integrated quantum photonics.

Bundulis Arturs[1]
[1] *Institute of Solid State Physics, University of Latvia*
E-mail: arturs.bundulis@cfi.lu.lv

Quantum light sources – either single-photon or entangled photons – are one of the major elements to enable quantum photonic applications. While there exist various photonic platforms that are slowly shifting to quantum applications (Si photonics, InP and others) no single platform encompass all the necessary quantum elements, mainly due to material limitations. An alternative approach is using hybrid-platform photonics, to combine strengths of multiple materials to counter their weaknesses. Here the main issue is the compatibility between different inorganic materials and the possibility to combine their workflows. Polymer photonics offers a solution to this issue by having high nonlinear optical efficiency and possibility to combine them in host-guest systems with polymers. Also, the possibility to create organic thin-films using wet-coating methods allows for simple integration with other quantum photonic platforms.

In ISSP we are working on new material selection for quantum applications, establishing workflows for device fabrication and designing devices. This talk will include newest results regarding nonlinear optical dyes and organic quantum emitters, characterization of their optical properties, quantum light source designing, and fabrication based on on-chip waveguides as well as new emerging directions enabled by unique properties of organic dyes.

Multimode fused silica optical fibers and fiber bundles at Lightguide

Grūbe Jurģis[1]

[1] *Lightguide, Celtniecibas street 8, Livani, LV-5316 Latvia*

Lightguide is a dynamic and competitive European-based company that develops, manufactures and supplies optical fibers, fiber bundles, cables and laser delivery systems for cutting-edge, highly sophisticated scientific, industrial and medical applications worldwide. With a team of 270+ bright-minded professionals, we have the expertise to invent and develop custom solutions that will set your business apart from the competition.

In this presentation I will give brief introduction about company and our products: multimode fused silica optical fibers and fiber bundles and our capabilities for custom solution for individual customers. The presentation will cover also various factors that can affect the applicability of fibers and fiber bundles.

Design and synthesis of nanophotonic materials via chemical solution synthesis

Hamawandi Bejan[1,2]
[1] *Institute of Solid State Physics, University of Latvia*
[2] *KTH Royal Institute of Technology*

Scalable synthetic approaches for high-quality and reproducible nanomaterials are essential for advancing the technologies. Here, we present a bottom-up wet chemical synthesis method as a cost-effective method to fabricate and scale up materials synthesis for nanophotonic applications.

The approach presents a rapid and energy-effective method for synthesizing silver nanoparticles and carbon-based quantum dots with promising optical and photonic properties. The wet chemistry methodology is based on understanding the chemical reactions' thermodynamics and the kinetics of the formation of nanomaterials. Additionally, it introduces an energy-effective volume heating using microwaves, leading to highly crystalline nanomaterials in a reaction duration of several minutes. Solvents like ethylene glycol and water with a high dielectric constant are suitable for synthetic processes providing greener reaction media.

Silver nanoparticles exhibit plasmonic properties, which involve the interaction of an electromagnetic field with the free electron cloud of the nanoparticles, resulting in resonance and enhancement of light in a specific wavelength. Carbon quantum dots are carbon-based nanoparticles with sizes typically less than a few nanometers, exhibiting fluorescence due to the interaction with electromagnetic lights. These characteristics make them promising candidates for different nanophotonic applications.

In terms of sustainability of the synthetic methodologies, energy and time efficiency, scalability, and the environmental impact of the synthetic processes are essential factors in paving the way for the broader impact of these synthetic strategies for developing promising strategic nanomaterials.

Creativity? Why?

Siliņa Dace
University of Latvia Career Centre

Creativity? How to understand it? Why do I have to be creative – I am not a painter?

This seminar will explore the power of creativity in creating a successful career and life – how to find your creativity and how to apply it in your life.

Visual functions in children with reading disorders

Ceple Ilze[1,*], Alecka Madara[1], Berzina Asnate[1], Goliskina Viktorija[1], Kassaliete Evita[1], Klavinska Anete[1], Koleda Marija[1], Mikelsone Rita[1], Ozola Elizabete[1], Ruza Tomass[1], Serpa Evita[1], Svede Aiga[1], Toloka Daniela[1], Truksa Renars[1], Vasiljeva Sofija[1], Volberga Liva[1], Krumina Gunta[1]

Department of Optometry and Vision Science, Faculty of Physics, Mathematics and Optometry, University of Latvia, Riga, Latvia

[*] *E-mail:* ilze.ceple@lu.lv

Reading is a visual task during which meaningful information is perceived through the dynamic interaction among the reader's existing knowledge, the information suggested by the written language, and the context of the reading situation (Reading Redefined: A Michigan Reading Association Position Paper, 2006). The prevalence of reading difficulties in school-aged children varies between 5-25%, depending upon the testing method applied, as well as the severity or cut-off applied for identification [1-3]. From optometrist's perspective, reading difficulties may be associated with poor visual acuity, unstable binocular vision, accommodative dysfunction, different ocular diseases or oculomotor dysfunction [4]. Specific learning disorders (including dyslexia) can also be associated with oculomotor abnormalities: reduced performance in anti-saccade and vertical saccade tasks, smooth pursuit eye movements, as well as reduced fixation stability [5-10].

Over the last years, we have been working intensively on a project aiming to explore the relation of visual and oculomotor functions and reading performance. Currently, at the final and the most intensive part of data analysis, we are finally connecting the dots and seeing the bigger picture. This is what I love about science – accurate and hard work leading to moments of revelation. In this talk I would like to share how we came to the current research idea, what we have done and discovered so far and what are our future plans on understanding the visual system and its role in successful reading performance.

Acknowledgements

This work has been supported by the Latvian Council of Science (project Nr.lzp-2021/1-0219), University of Latvia (project Nr. Y5-AZ77-ZF-N-100) and SIA Mikrotikls and the University of Latvia Foundation (project Nr. 2260).

References

[1] Wagner, R. K., Zirps, F. A., Edwards, A. A., Wood, S. G., Joyner, R. E., Becker, B. J., Liu, G., & Beal, B. (2020). The Prevalence of Dyslexia: A New Approach to Its Estimation. Journal of Learning Disabilities, 53(5), 354-365.

[2] Yang L, Li C, Li X, Zhai M, An Q, Zhang Y, Zhao J, Weng X. (2022). Prevalence of Devel-

opmental Dyslexia in Primary School Children: A Systematic Review and Meta-Analysis. Brain Sciences. 12(2), 240.
[3] Cecilia, M.R., Vittorini, P., Cofini, V., di Orio, F. (2014). The prevalence of reading difficulties among children in scholar age. Styles of Communication, 6(1), 18-30.
[4] Christian, L.W., Nandakumar, K., Hrynchak, P.K., Irving, E.L. (2018). Visual and binocular status in elementary school children with a reading problem. Journal of Optometry, 11(3), 160-166.
[5] Jafarlou, F., Jarollahi, F., Ahadi, M., Sadeghi-Firoozabadi, V., Haghani, H. (2017). Oculomotor rehabilitation in children with dyslexia. Medical Journal of the Islamic Republic of Iran, 31, 125. [6] Lukasova, K., Silva, I. P., & Macedo, E. C. (2016). Impaired Oculomotor Behavior of Children with Developmental Dyslexia in Antisaccades and Predictive Saccades Tasks. Frontiers in psychology, 7, 987.
[7] Jothi Prabha, A., Bhargavi, R. (2020). Predictive Model for Dyslexia from Fixations and Saccadic Eye Movement Events. Computer Methods and Programs in Biomedicine, 195.
[8] Nilsson Benfatto, M., Öqvist Seimyr, G., Ygge, J., Pansell, T., Rydberg, A., & Jacobson, C. (2016). Screening for Dyslexia Using Eye Tracking during Reading. PloS One, 11(12).
[9] Bilbao, C., Pinero, D.P. (2020). Clinical Characterization of Oculomotricity in Children with and without Specific Learning Disorders. Brain Sciences, 10(11), 836.
[10] Bilbao, C., Piñero, D.P. (2021). Objective and Subjective Evaluation of Saccadic Eye Movements in Healthy Children and Children with Neurodevelopmental Disorders: A Pilot Study. Vision (Basel, Switzerland), 5(2), 28.

Part II
Talks

SPIE. STUDENT CHAPTER UNIVERSITY OF LATVIA

UNIVERSITY OF LATVIA

82nd International Scientific Conference of the University of Latvia 2024

UNIVERSITY OF LATVIA
INSTITUTE OF ATOMIC PHYSICS AND SPECTROSCOPY

Investigating the solution-processible organic cross-linkable materials for hole transport layer of OLED

Tetervenoka Natalija[1,*], Stucere Kitija Alise[1], Vaitukaityte Deimante [2], Vembris Aivars[1]

[1] *Institute of Solid State Physics, University of Latvia, Latvia*
[2] *Department of Organic Chemistry, Kaunas University of Technology, Lithuania*
[*] *E-mail:* natalie@cfi.lu.lv

At present, organic light-emitting diodes (OLEDs) are widely regarded as the optimal technological choice for achieving high-quality displays[1]. Because of this swiftly evolving field, it is required to introduce novel materials and technologies that have the potential to lower costs and enhance device performance. One of the options is the use of solution-processible organic cross-linkable materials in the hole transport layer (HTL) in OLED which eliminates the necessity of orthogonal solvents in wet-coating processes and reduces the need for expensive vacuum technologies[2].

In this work, two solution-processible enamine-based cross-linkable materials V1162 and V1187 were studied. A cross-linking process was realized by thermal annealing of the films at a glass transition temperature making them insoluble[3]. Afterwards, subsequent layers were applied. The results were compared with conventionally used PolyTPD.

The experiments were divided into three sets. In the first set, the novel compounds were compared to the PolyTPD. In the second and third different concentrations of V1162 and V1187 respectively were analysed.

The attained results showed that using novel materials, despite a slightly higher turn-on voltage, it is possible to achieve almost 4 times higher maximum luminance and significantly higher external quantum, current and power efficiencies in different luminance ranges.

The new materials are competitive not only because of their performance, but also because of their relatively low cost, however, further optimisation of the OLED stack may be applied.

References

[1] Chen, H.-W., Lee, J.-H., Lin, B.-Y., Chen, S. & Wu, S.-T. Liquid crystal display and organic light-emitting diode display: present status and future perspectives. Light Sci. Appl. 7, 17168–17168 (2017).

[2] Handbook of Organic Light-Emitting Diodes. (Springer Japan, 2020). doi:10.1007/978-4-431-55761-6

[3] Kim, T.-Y., Jung, J.-H., Kim, J.-B. & Moon, D.-G. Achieving high efficiency by high temperature annealing of hole transporting polymer layer in solution-processed organic light-emitting devices. Synth. Met. 232, 167–170 (2017).

Sulfonyl functionalization for improving TADF rate in carbene-metal-amide complex

Stucere Kitija A.[1,*], Ruduss Armands[2], Jece Annija[2], Chen Kuan-Wei[3], Turovska Baiba[4], Belyakov Sergey[4], Vembris Aivars[1], Chang Chih-Hao[3], Traskovskis Kaspars[2]

[1] *Institute of Solid State Physics, University of Latvia*

[2] *Institute of Applied Chemistry, Riga Technical University*

[3] *Department of Electrical Engineering, Yuan Ze University*

[4] *Latvian Institute of Organic Synthesis*

[*] *E-mail:* kitija@cfi.lu.lv

The demand for low cost, more efficient and functional illumination continues to grow. Organic light-emitting diodes (OLEDs) make it possible to produce flexible displays with high color quality and relatively low power consumption comparing to alternatives, yet a good light emitter is needed for high-quality OLEDs. Carbene-metal-amide (CMA) complexes are robust compounds with fast emission lifetimes and near-unity photoluminescence quantum yields. However, their structural diversity is largely limited by the small number of suitable carbene fragments possessing sufficient stability and π-accepting property.

In this work, a CMA complex was synthesized and investigated. The compound was modified with sulfonyl group, enabling efficient thermally activated delayed fluorescence (TADF) comparing to long-lived phosphorescence in sulfone-free analogous compounds. Photoluminescence and emission lifetime measurements for 5wt% PMMA thin films in different temperatures were conducted, followed by fabrication and testing of OLEDs.

In this compound an optimal electronic configuration was attained, resulting in efficient green TADF emission characterized by the very high radiative rate - $1.3 \cdot 10^6 s^{-1}$ and photoluminescence quantum yield of 0.85, as well as low singlet-triplet energy gap - 0.05 eV. Fabricated OLEDs external quantum efficiency reached 8.6%, maximum luminance 26 000 cd/m^2, showing the practical usability of the compound.

Third- and higher order nonlinear optical properties of organic materials

Berzina Anete[1,*], Bundulis Arturs[1]
[1] *Institute of Solid State Physics, University of Latvia*
[*] *E-mail:* anete.berzina@cfi.lu.lv

The advancement of modern communication systems has increased the necessary data transmission bandwidth and has sparked interest in optical signal processing devices. Research of developing such devices is focused on finding materials with high nonlinear optical (NLO) efficiency. In such research organic materials are being investigated more frequently due to the possibility of modifying the molecular structure to influence nonlinear response. In organic materials higher NLO efficiencies have been observed and they could be used in the development of lower power photonic devices.

In this work, reference measurements with organic solvents (anisole, chloroform, CS2) for system calibration were performed and solutions were prepared with chloroform and glass-forming azochromophore compounds.

The solutions were irradiated with a tunable femtosecond laser in the range of 400-1100nm using the z-scan method. Approaching the ultraviolet region of the spectrum during reference measurements, anisole exhibited properties indicative of third- and fifth-order effects.

Based on the experimental results, the effectiveness of NLO properties of organic materials and their application possibilities in polymer photonics was evaluated.

Acknowledgments

This work is done in the frame of National research program VPP-EM-FOTONIKA-2022/1-0001 "Smart Materials, Photonics, Technologies and Engineering Ecosystem".

MODELING FERMI RESONANS IN CO2 MOLECULE USING NATURAL COORDINATES

Kachkina Daria[1,*], Khursevich Nikita[1], Malevich Alex[1], Pitsevich George[1]
[1] *Belarusian State University, Minsk, Belarus*
[*] *E-mail:* spooky.alien@mail.ru

The carbon dioxide (CD) molecule plays an important role in atmospheric processes, contributes to the formation of the greenhouse effect and is widely present in the atmospheres of other planets of the solar system and exoplanets. The CO_2 molecule is also found in gaseous nebulae of interstellar space and in many comets. Carbon dioxide is one of the simplest linear molecules and belongs to the point symmetry group $D_{\infty H}$. The CO_2 molecule has long been the focus of attention of researchers, both theoreticians and experimentalists, to this day. However, the description of bending vibrations in this molecule remains incomplete and requires a more detailed consideration.

It is well known that the overtones of bending vibrations in this molecule are perturbed by the Fermi resonance caused by interaction with the totally symmetric stretching vibration of C=O bonds. For a correct description of this resonance, the choice of vibrational coordinates plays a crucial role. A recent attempt to use Cartesian coordinates as vibrational ones to describe all vibrational modes of a molecule failed to model Fermi resonances [1]. It is obvious that taking into account all vibrational degrees of freedom is possible only with the help of a complete set of generalized natural coordinates. To be able to describe the analyzed mode using two natural deformation coordinates ϕ_1, ϕ_2, the values of which in the equilibrium configuration are taken equal to 180°, the following geometric relationship (1) was used, connecting the simultaneous deformation of the molecule in two orthogonal planes at angles ϕ_1 and ϕ_2 with the angle ϕ determining the resulting bent configuration of the molecule (see Fig. 1):

$$cos^2\frac{\phi}{2} = cos^2\frac{\phi_1}{2} + cos^2\frac{\phi_2}{2}; \tag{1}$$

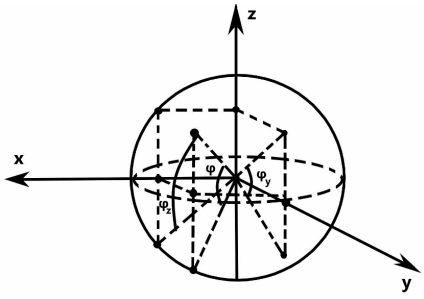

Figure 1: Relationship between the simultaneous deformation of a molecule in two orthogonal planes by angles ϕ_1 and ϕ_2 with the angle ϕ that determines the resulting bent configuration of the molecule.

Table 1: Calculated at the CCSD(T)/acc-pVQZ level of theory, the energy values of stationary deformation vibrations of the CO_2 molecule with an anharmonic 2D potential energy surface.

Number of energy level	Quantum numbers		Energy [cm^{-1}]	Energy [cm^{-1}]
	n_2	l_2	E_{calc}	E_{exp}
1	0	0	0	0
2	1	+1	667.19	667.77
3	1	-1	667.19	667.77
4	2	0	1332.73	1285.41
5	2	+2	1334.88	1336,67
6	2	-2	1334.88	1336,67
				1388,21
7	3	+1	1999.32	1932.86
8	3	-1	1999.32	1932.86
9	3	+3	2005.05	2006.77
10	3	-3	2005.05	2006.77

The two-dimensional vibrational Schrödinger equation using these coordinates takes the following form:

$$-2(A - Bcos\phi_1)\frac{\partial^2\Psi}{\partial\phi_1^2} - 2(A - Bcos\phi_2)\frac{\partial^2}{\partial\phi_2^2} + U(\phi_1, \phi_2)\Psi = E\Psi; \quad (2)$$

Potential energy U(ϕ_1, ϕ_2) was calculated at CCSD(T)/Aug-cc-pVQZ level of theory. Equation (2) was solved numerically using the DVR method. The results are presented in Tabl. 1

Let us recall that the vibrational state of the CO2 molecule can be described by a set of four quantum numbers (n_1,n_2,l_2,n_3),, where n_1 characterizes the totally symmetric stretching vibration of C=O bonds, n_2 and l_2 are the doubly degenerate bending vibration and n_3 is the antisymmetric stretching vibration of C =O bonds. Since the last mode is not considered in this work, only the first three quantum numbers are used in what follows.

To simulate the Fermi resonance, a totally symmetric valence coordinate l was additionally introduced. In this case, the kinetic energy operator took the following form:

$$-2(A - Bcos\phi)\frac{\partial^2\Psi}{\partial l^2} - \frac{2}{l^2}[\ (A - Bcos\phi_1)\frac{\partial^2\Psi}{\partial\phi_1^2} + (A - Bcos\phi_2)\frac{\partial^2}{\partial\phi_2^2}]\ - \frac{4B}{l}[\ sin\phi_1\frac{\partial^2}{\partial l\partial\phi_1} + sin\phi_2\frac{\partial^2}{\partial l\partial\phi_2}]\ ; \quad (3)$$

The numerical solution of the Schrödinger equation with such a kinetic energy operator gives the following values of the energies of vibrational levels (see Table 2):

As can be seen from the results of Table 2, using natural coordinates it is possible to correctly describe not only vibrational modes that are not involved in Fermi resonances, but also vibrational states perturbed by the Fermi resonance. In this case, the calculated values of the splitting values due to the Fermi resonance are in good agreement with the experimental values. Symmetry restrictions on interacting energy levels are also analyzed.

Table 2: Calculated at the CCSD(T)/acc-pVQZ level of theory, the energy values of stationary bending vibrations of the CO_2 molecule with an anharmonic 3D potential energy surface, taking into account the symmetrical stretching vibrations of C=O bonds.

Number of energy level	Quantum numbers			Energy [cm^{-1}]	Energy [cm^{-1}]
	n_1	n_2	l_2	E_{calc}	E_{exp}
1	0	0	0	0	0
2	0	1	+1	667.03	667.77
3	0	1	-1	667.03	667.77
4	1 0	0 2	0 0	1282.37	1285.41
5	0	2	+2	1334.88	1336,67
6	0	2	-2	1334.88	1336,67
7	1 0	0 2	0 0	1392.94	1388.21
8	1 0	1 3	+1 +1	1930.48	1932.86
9	1 0	1 3	-1 -1	1930.48	1932.86
10	0	3	+3	2005.05	2006.77
11	0	3	-3	2005.05	2006.77
12	1 0	1 3	+1 +1	2079.31	2076.55
13	1 0	1 3	-1 -1	2079.31	2076.55

References

[1] Liang, Z., Tsai, H.-L., Determination of vibrational energy levels and transition dipole moments of carbon dioxide molecules by density functional theory, Journal of Molecular Spectroscopy, 252 (2008) 108-114

Study of semiconductor surface nanostructuring with vector laser beams

Kalnins Kalvis[1]

[1] *Institute of Atomic Physics and Spectroscopy, University of Latvia, Jelgavas 3, Riga*

[*] *E-mail:* kalvis.kalnins.lu@lu.lv

When a material's surface is exposed to laser irradiation, it can lead to the formation of Laser-Induced Periodic Surface Structures (LIPSS). These structures manifest as periodic lines on the surface and demonstrate a distinct correlation with the polarization and wavelength of the incident beam.

In this research, we explore the changes in surface structures of semiconductors under irradiation by a vector beam. This vector beam is generated utilizing an S-wave plate, which converts a linearly polarized laser beam into a helical beam with radial or azimuthal polarization, dependent upon the angle of the S-wave plate.

We found optimal parameters for producing LIPSS on silicon and gallium arsenide wafers through experimentation. By manipulating polarization states (linear, radial, azimuthal, and a blend achieved via S-wave plate adjustment), we created nanostructures, which we analysed the nanostructures using SEM images.

We used 30 ps 532 nm laser pulses for our experiments. Employing the S-Waveplate, we transformed the laser beam into a helical beam with the desired polarization and focused it onto the surface of the target material using a 1000mm lens. We determined the optimal laser pulse count and fluence to achieve the best nanostructures. Additionally, a camera positioned in the focal plane of the beam allowed us to visualize the beam profile and calculate the area of irradiated surface.

We've noted an unconventional alignment of nanostructures, where they align parallel to the polarization direction. This is interesting as LIPSS typically exhibit a perpendicular orientation relative to the polarization.

Acknowledgments

We would like to express our sincere gratitude to R.A. Ganeev, V.V. Kim, for guiding the work and discussions. Work was supported by Fundamental and Applied Research Project (Nr. lzp-2023/1-0199): "The Laser Photodetachment Spectroscopy on Negative Ions", from Latvian Science Council.

Splitting of magneto-optical double resonance absorption peaks at high RF intensity

Seržane-Sadovska Linda [1,*], Mozers Artūrs[1], Gahbauer Florian[1], Auzinsh Marcis[1]
[1] *Laser Centre, University of Latvia, Raina Boulevard 19, LV-1586 Riga, Latvia*
[*] *E-mail:* ls16175@lu.lv

In this work, the effect of radio frequency (RF) intensity on magneto-optical absorption signals in the 133Cs atoms was experimentally studied. As the present study is a part of a project with the intent to develop a method for magnetic field sensing in three orthogonal directions by using only two linearly polarized beams, here we use linearly polarized excitation contrary to the commonly used circularly polarized excitation.

A longitudinal alignment is created when atoms absorb linearly polarized light. Next, a shift in the energy of magnetic sublevels is caused by applying an external magnetic field parallel to the linearly polarized excitation. If, additionally, a RF field is applied in resonance with the splitting of magnetic sublevels, then the population will be redistributed among the neighboring magnetic sublevels. As the magnetic field is being scanned while the applied RF field remains constant the absorption signal changes because at particular magnetic field values the population returns to magnetic sublevels with larger transition probability.

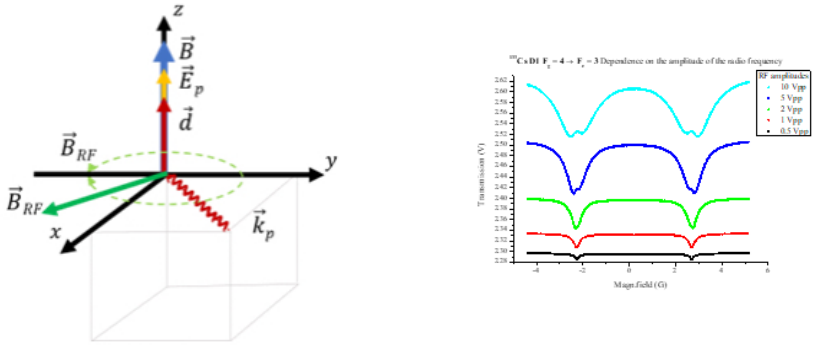

Figure 1: (a) The geometry for measuring the RF double-resonance absorption signal. (b) The transmission signal dependence on magnetic field for different amplitude values of RF with laser frequency fixed to the ^{133}Cs D1 $Fg_4 \rightarrow Fe_4$ transition

To implement this experimentally we used the following geometry (see Fig.1a): the quantization axis is parallel to the direction of the magnetic field (B), a linearly polarized laser beam (Ep) is applied along the quantization axis and the oscillating RF field (BRF) can be split into two circular radio frequency components that are located in the x-y plane perpendicular to B.

We collected dependencies of absorption signals on several experimental parameters: RF intensity, RF value, laser frequency, laser intensity and laser beam diameter. In figure 1b an increase in the signal amplitude can be observed as the RF intensity increases. Furthermore, an additional structure appears for large RF intensities, specifically, a change in the direction of the absorption peak can be observed. Another way of interpreting the observed signals is in terms of the peak being split by the larger RF fields. This may be related to a process similar to the Autler-Townes splitting.

Acknowledgments

We acknowledge the support from the Latvian Council of Science, project No. lzp-2020/1-0180: "Compact 3-D magnetometry in Cs atomic vapor at room temperature"

Autofluorescence imaging and autofluorescence photobleaching imaging of basal cell carcinoma lesions in basal cell nevus syndrome patients

Plorina Emilija Vija[1,*], Lihachev Alexey[1], Kiss Norbert[2], Bliznuks Dmitrijs[3], Lihacova Ilze[1]

[1] *Institute of Atomic Physics and Spectroscopy, University of Latvia, LV-1586 Riga, Latvia;*

[2] *Department of Dermatology, Venereology and Dermatooncology, Semmelweis University, Maria str.41., H-1085 Budapest, Hungary;*

[3] *Institute of Smart Computing Technologies, Riga Technical University, Zunda krastmala 10, LV-1658 Riga;*

[*] *E-mail:* plorina@lu.lv

Basal cell carcinoma (BCC) is the most common type of cancer in the general population and its incidence is increasing by up to 10% per year [1]. Basal cell nevus syndrome (BCNS) is a rare autosomal dominant disorder that increases predisposition to basal cell carcinoma [2]. The estimated prevalence according to the international database on rare diseases is between 1 in 31 000 to 1 in 164 000 people [3]. Autofluorescence and autofluorescence photobleaching imaging is a potential approach to early diagnosis of BCC [4], however, the mechanism is still not fully understood. By studying BCC autofluorescence in people with BCNS, the way to diagnose these lesions at an early stage may be discovered. The goal of this study was to analyze autofluorescence imaging and autofluorescence photobleaching imaging data of BCC from general population and BCC from BCNS patients and determine how autofluorescence parameters are characterized in BCC from both of these groups.

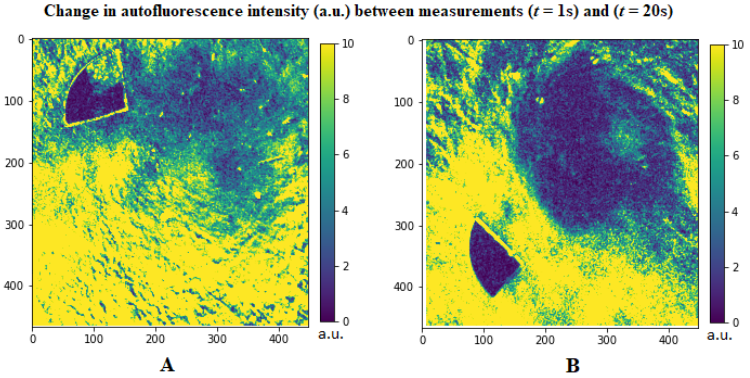

Figure 1: Maps of absolute autofluorescence intensity change between the first and last measurement at the start and end of measurements for general BCC (A) and BCC in a patient with BCNS (B).

A custom imaging device with 405 nm LED illumination was used for inducing cutaneous autofluorescence, a 515 nm long-pass filter over the camera lens for filtering out the excitation wavelength, polarizing filters for reducing glare and CMOS sensor for capturing imaging data. With continuous irradiation of 20 seconds, the autofluorescence photobleaching imaging data was detected. Data processing was conducted using the Python programming language. Results show that BCC in patients with BCNS has a lower autofluorescence intensity at the first second of excitation, as well as smaller decrease in intensity after 20 seconds compared to BCC from other patients. Examples of maps for change in autofluorescence intensity depending on the patient group are shown in Figure 1. This may show that BCC in patients with BCNS has a different morphology and composition of fluorescent molecules which should be investigated further.

Acknowledgement
This research was supported by Latvian Council of Science project Non-melanoma skin cancer diagnostics by evaluating autofluorescence photobleaching kinetics (Nr. lzp-2022/1-0255).

References
[1] Christenson LJ, Borrowman TA, Vachon CM, Tollefson MM, Otley CC, Weaver AL, Roenigk RK. Incidence of basal cell and squamous cell carcinomas in a population younger than 40 years. JAMA. 2005 Aug 10;294(6):681-90. doi: 10.1001/jama.294.6.681. PMID: 16091570.
[2] Joshi PS, Deshmukh V, Golgire S. Gorlin-Goltz syndrome. Dent Res J (Isfahan). 2012 Jan;9(1):100-6. doi: 10.4103/1735-3327.92963. PMID: 22363371; PMCID: PMC3283966.
[3] Lo Muzio L. (2019, May), Gorlin syndrome, https://www.orpha.net/en/disease/detail/377 (accessed on 20 March 2024).
[4] A. Lihachev, E. V. Plorina, M. Lange, I. Lihacova, A. Derjabo, and D. Bliznuks, "Imaging of LED-excited autofluorescence photobleaching rates for skin lesion diagnostics," in Clinical and Preclinical Optical Diagnostics II, Vol. EB101 of SPIE Proceedings (Optica Publishing Group, 2019), paper 11073 63.

Eye vergence training options

Kosona Anastasija[1,*], Bisofa Anda[1], Jakovica Anastasija[1], Eigusa Krista[1], Vercinska Emija[1], Krumina Gunta[1]

[1] *University of Latvia, Department of Optometry and Vision Science*

[*] *E-mail:* anastasija.kosona@lu.lv

The proliferation of smart devices in contemporary society not only facilitates daily activities but also imposes an additional strain on the visual system. Research indicates that children are commencing usage of smart devices as early as 1-2 years of age, implying a growing risk of visual impairments among the younger population due to prolonged device usage [1]. Proximal tasks emerge as a prominent factor disrupting visual equilibrium, potentially leading to visual discomfort and the onset of vision disorders. Such impairments and discomfort are observable across various age groups, encompassing preschoolers, school-age children, and adults alike [2]. The aim of the study was to investigate the literature on eye-vergence training and to evaluate the developed eye vergence training game "Bulta".

Studying the literature we saw that there is manual, vectograph, as well as computerized vision training. Over time, manual and vectograph vision training is losing its popularity. Computerized ones solve many of the above-mentioned problems of vision training, for example, maintaining the patient's interest during the training, which significantly affects the effectiveness and results of the training. Our investigation revealed notable enhancements in eye vergence parameters over the course of the six sessions, marked by an augmentation in both convergent fusional maximum and divergent fusional maximum. It's worth noting that the initial divergent fusional reserve was relatively smaller, thus limiting the potential increase in the maximum magnitude of this specific type of vergence. Furthermore, our assessment during the "Bulta" game training sessions indicated a reduction in response time, underscoring the efficacy of the training regimen.

After studying the literature, we came to the conclusion that convergence insufficiency is the most common vergence disorder and basically vision training is based on the possibilities of preventing this disorder. Through our iteration of the game, we have demonstrated the capacity to train eye vergence. Our findings reveal consistent improvements across successive game sessions, characterized by an increase in maximum fusional vergence alongside a reduction in response time.

References

[1] Chang H Y et al. Electronic Media Exposure and Use among Toddlers. Psychiatry Investigation, 15(6), 568-573, (2018).

[2] Wang J et al. Smartphone Overuse and Visual Impairment in Children and Young Adults: Systematic Review and Meta-Analysis. J Med Internet Res, 22(12), e21923, (2020).

Myopia screening method based on computer vision analysis of retinal fundus pictures: The effect of image size

Rizzieri Nicola[1,*], Dall'Asta Luca[2], Ozolinsh Maris[1]
[1] *University of Latvia, Faculty of Physics, Mathematics and Optometry, Department of Optometry and Vision Science, Riga, Latvia*
[2] *LIFE Srl, Research and Development, Bari, Italy*
[*] *E-mail:* nirizzieri@gmail.com

Myopia is of global concern due to its increasing prevalence worldwide and its potential for side eyethreatening conditions such as myopic maculopathy, glaucoma, cataracts and retinal detachment. Cycloplegic refraction, distance visual acuity and, more recently, the measurement of axial length are the diagnosis standards. Screening programs focused on myopia detection usually involve one or more tests, requiring skilled and well-trained examiners, longer chair time, and only sometimes child-friendly. Recently, the application of artificial intelligence techniques, such as computer vision, in the medical field has increased the availability of robust screening and diagnostic tools. This opportunity needs to be further investigated when it comes to myopia detection. We developed and tested an objective method to detect myopia directly from retinal fundus pictures. We trained a YOLOv8-based neural network to immediately recognise myopic and non-myopic retinographies, reaching an overall model accuracy of 85%, specificity and sensitivity of 75% and 88.33%, respectively. By changing the size of the input images from 640x640 to 1024x1024 pixels, the performance metric specificity decreased to 50% while the sensitivity increased to 96.67%. We developed a promising model that could be implemented for onsite or distance screening programs, reducing the need for expert practitioners and time-consuming clinical tests. Further improvements, such as proper input image size, batch size, and computational load, should be considered to correctly balance sensitivity and specificity to set desired conditions for using this method efficiently and accurately in clinical practice.

Common vision problems and their impact on user experience and performance in a VR environment

Krastina Ieva[1,*], Svarverud Ellen[1], Gilson Stuart J.[1], Baraas Rigmor C.[1], Hagen Lene A.[1]

[1] *National Centre for Optics, Vision and Eye Care, Faculty of Health and Social Sciences, University of South-Eastern Norway, Kongsberg, Norway*

When using virtual reality (VR) technologies, users rely greatly on their vision to navigate in the virtual environment. Despite this, there is a gap in current research on how common vision problems might affect performance and individual experience during and after VR use. Vision problems, poor sensorimotor ability, and cybersickness may act as barriers to adopting VR technologies.

The study aims to assess whether and how common vision problems affect user experience and performance in a VR environment. It also explores the impact of visual function and postural control on accessibility and user experience in VR.

The participants were adolescents recruited from one upper secondary school in South-East Norway. Baseline measurements were obtained from a comprehensive set of spatial and binocular vision tests, and cycloplegic refractive error was measured. Postural sway was recorded using a smartphone-based accelerometer worn at waist level while the participant was asked to do five balance poses to evaluate the impact of vision, proprioceptive and vestibular systems on posture control. The participants then played a VR game (Beat Saber) in a Pico Neo 2 Eye headset, for 10 and 30 minutes, and repeated the balance tests immediately afterwards to assess postural control before and after VR gaming. Finally, participants completed a virtual reality cyber sickness questionnaire and repeated some of the vision tests to assess changes in discomfort and vision. Future analyses will explore how participants with common vision problems experience challenges in the VR environments, and whether common vision problems may affect post-VR postural control. Understanding the diversity in common vision problems and its connection to eye-body coordination may inform more inclusive designs of VR, enhancing accessibility and user experience.

Part III
Poster Session

SPIE. STUDENT CHAPTER UNIVERSITY OF LATVIA

UNIVERSITY OF LATVIA

82nd International Scientific Conference of the University of Latvia 2024

UNIVERSITY OF LATVIA
INSTITUTE OF ATOMIC PHYSICS AND SPECTROSCOPY

EFFECT OF ASSOCIATION ON OPTICAL ROTATION AND NON LINEAR PROPERTIES OF LIQUID CRYSTAL N4OYBDHA MOLECULE

Dziubkina Elena[1,*], Eremenko Polina[1], Galinskaya Darya[1], Pitsevich George[1]
[1] *Belarusian State University, Minsk, Belarus*
[*] *E-mail:* lena.dyubkina@mail.ru

The phenomenon of optical activity of certain molecular media is of great interest, since it is successfully used in many technical applications and plays an important role in biological processes, as well as in modeling the properties of drugs. Their non-linear optical properties play an equally important role. It is well known that optical activity is inherent in molecules that have the property of chirality, i.e. having mirror analogues or structural fragments possessing this property. However, the medium assumes that several identical molecules are involved in the interaction with the light wave. Therefore, in this work we study the dependence of the characteristics described above on the number of associated liquid crystal (LC) molecules.

For this purpose, the configurations of the monomer, two conformers of the dimer, and the trimer of the N4OYBDHA LC molecule were optimized at the B3LYP/STO-3G, B3LYP/3-21G, and B3LYP/6-311G levels of theory. Optimized configurations are shown in Fig. 1

Figure 1: From left to right – theoretically optimized B3LYP/3-21G configurations of the monomer, dimer I, dimer II and trimer of the N4OYBDHA LC molecule.

Then, nonlinear optical characteristics were calculated for all associates at the B3LYP/3-21G level of theory. In particular, Table 1 presents some invariants and components of the cubic tensor of the first hyperpolarizability. As follows from the data in Table 1, the non-linear optical characteristics of the associates are not the sum of the corresponding characteristics of the monomers, which indicates a significant interaction between the electronic shells of LC molecules

Then the optical activity of the monomer and associates was calculated at the B3LYP/3-21G level of theory for several wavelengths of incident radiation. As is known, the most important characteristic that determines the efficiency of optical activity is the value $|\alpha|\lambda$, which characterizes the angle of rotation of the plane of polarization of a light wave in degrees per one decimeter of layer thickness, one gram of substance and one cubic centimeter of volume. The calculation results are presented in Table 2.

According to the data in Table 2, the angle of rotation of the plane of polarization increases with decreasing wavelength. However, for dimer I the situation is opposite. The same dimer is characterized by an increase in the angle of rotation for some wavelengths

Table 1: Values of components and invariants of the cubic tensor of the first hyperpolarizability of monomer conformers, two dimer conformers, and trimer of an LC molecule in vacuum, calculated at the B3LYP/3-21G level of theory. Results are presented in atomic units

Associate									
Monomer	$\beta_{\parallel}(z)$	$\beta_{\perp}(z)$	β_x	β_y	β_z	$\beta_{\parallel}$	β_{xxx}	β_{xxy}	β_{yxy}
	-723,2	-241,1	-37,7	-1270,1	-3774,3	766,6	20,5	7,2	7,5
	β_{yyy}	β_{zxz}	β_{xxx}	β_{yxz}	β_{yyz}	β_{zyz}	β_{zzz}		
	-56,5	36,5	-0,2	-168,5	-40,5	-374,1	-1073,3		
Dimer I	$\beta_{\parallel}(z)$	$\beta_{\perp}(z)$	β_x	β_y	β_z	$\beta_{\parallel}$	β_{xxx}	β_{xxy}	β_{yxy}
	-138.2	-46.1	-2756.7	-1243.8	-691.3	620.4	-882.3	-344.7	-140.7
	β_{yyy}	β_{zxz}	β_{xxx} β_{yxz}		β_{yyz}	β_{zyz}	β_{zzz}		
	-127.8	-112.3	-35.7		-17.2	104.1	57.9	-100.9	
Dimer II	$\beta_{\parallel}(z)$	$\beta_{\perp}(z)$	β_x	β_y	β_z	$\beta_{\parallel}$	β_{xxx}	β_{xxy}	β_{yxy}
	-506.1	-168.7	-737.0	-795.6	2530.8	550.7	16.0	-16.2	-79.5
	β_{yyy}	β_{zxz}	β_{xxx}	β_{yxz}	β_{yyz}	β_{zyz}	β_{zzz}		
	-128.1	-155.8	33.0	-254.1	-182.1	-120.9	-433.7		
Trimer	$\beta_{\parallel}(z)$	$\beta_{\perp}(z)$	β_x	β_y	β_z	$\beta_{\parallel}$	β_{xxx}	β_{xxy}	β_{yxy}
	-190.1	-63.4	1354.1	-4159.4	-950.6	895.2	37.6	-164.1	421.1
	β_{yyy}	β_{zxz}	β_{xxx}	β_{yxz}	β_{yyz}	β_{zyz}	β_{zzz}		
	-1365.3	-76.2	32.9	-35.2	-7.3	143.0	-205.5		

by almost an order of magnitude, although during the transition from monomer to dimer II and to the trimer, a significantly smaller increase in the angle of rotation of the light wave plane is observed. Obviously, additional calculations are needed to establish the reason for these results.

Table 2: The value of the angle of rotation of the plane of polarization of the light wave $|\alpha|\lambda$ by the monomer, dimers and trimer of the LC molecule N4OYBDHA, calculated at the B3LYP/3-21G level of theory for four wavelengths.

	$\lvert\alpha\rvert\lambda$ [deg(dm·g/cm^3)$^{-1}$]			
	Red	Yellow	Green	Blue
	λ = 702 [nm]	λ = 577 [nm]	λ = 542 [nm]	λ = 475 [nm]
Monomer	-34.61	-51.03	-61.82	-84.69
Dimer I	-874.61	961.63	293.22	-193.98
Dimer II	-35.64	-52.58	-63.73	-87.34
Trimer	-87.73	-133.07	-165.85	-233.07

Acknowledgments

This study was supported by the Belarusian State Program of Scientific Investigations 2021–2025 "GPNI Chemical processes, reagents and technologies, bioregulators and bioorgchemistry" (2.1.01.04).

Spectral and thermal characteristics of pulsing a arsenic electrodeless lamp

Gudermanis Rolands[1]

[1] *Institute of Atomic Physics and Spectroscopy, University of Latvia, Riga, Latvia*

[*] *E-mail:* rolands.gudermanis@lu.lv

High-frequency electrodeless lamps (HFEDLs) are used in spectroscopy because of their characteristic narrow and intense spectral lines. Researching HFEDLs' properties is important to optimize them for usage in atomic absorption spectroscopy as well as to contribute to low-pressure, low-temperature inductively coupled plasma research.

In this work, I measured the spectral and thermal properties of arsenic-containing HFEDLs during self-modulation. Self-modulation is a phenomenon that occurs within HFEDLs with arsenic, selenium, iodine, bromine, chlorine, etc. filling at higher excitation generator power values. It can be observed as periodic pulses in spectral intensity.

Spectra for the arsenic containing HFEDL were registered with the OceanOptics HR4000 spectrometer, and thermal images were taken with the FLIR E75 infrared imaging camera. For data analysis, the OriginPro 2019b and FLIR tool programs were used.

Results have shown that for excitation generator voltage value of 17 volts, the arsenic-containing HFEDL temperature within a single pulse of self-modulation on average ranged from 320°C to 410°C. The results also show how spectra and temperatures are related during self-modulation.

SERS RESPONSE OF SILVER NANOPARTICLES DEPOSITED ON LASER-INDUCED PERIODIC SURFACE STRUCTURES

Mikalkevicius Mantas[1,*], Khinevich Nadzeya[1], Tamulevicius Tomas[1], Tamuleviciene Asta[1]

[1] *Institute of Materials Science of Kaunas University of Technology, K. Barsausko Str. 59, LT-51423, Kaunas, Lithuania*

[*] *E-mail:* mantas.mikalkevicius@ktu.lt

Raman spectroscopy is a very powerful nondestructive, label-free vibrational spectroscopic platform for molecular identification. The intrinsic drawback of this spectroscopy is that the scattering process is very inefficient and therefore the characteristic analyte signal intensities are very low. It requires a high-intensity light source, namely lasers, to detect low analyte concentrations. However, the signal can be enhanced chemically or electromagnetically introducing dedicated surface structures.
Generation of laser-induced periodic surface structuring (LIPSS) is a fast and low-cost method for nanostructure formation. LIPSS have potential benefits as a SERS substrate [1], where it was applied as a rough surface for plasmonic film deposition [2] or as a template for nanoparticle deposition.

In this work, chemically synthesized spherical silver nanoparticles of 100 nm diameter were deposited on silicon surface with LIPSS. LIPSS was formed using a fundamental harmonic (1030 nm) of a Yb:KGW femtosecond laser Pharos (Light Conversion) operating at a 200 kHz repetition rate with a pulse duration of 290 fs. The laser beam was scanned on the surface in straight lines with a 5 μm gap between the trajectories at 250 mm/s speed. The light polarization was 0 ° with respect to scanned lines. Nanoparticles were deposited on LIPSS by drop evaporation and monolayer formation methods. Drops were dried at 35 °C, 21 °C, and 4 °C temperatures. SERS response of 2-Naphthalenethiol (2NT) molecule was analyzed using Raman microscope inVia (Renishaw) equipped with 532 nm laser.

We have observed that Raman signal intensity depends on nanoparticle deposition method. The lowest signal was recorded for the drop dried at 35 °C temperature, while the highest intensity was achieved for a monolayer sample and characteristic peaks of 2-NT molecule were determined at 10^{-4} M concentration. Lowering the concentration we reach our limit of detection for monolayer sample at 10^{-7} M concentration. Calculated signal enhancement factor for silver nanoparticle monolayer was equal to $9.95 \cdot 10^5$.

References

[1] C.-H. Lin et al., "One-step fabrication of nanostructures by femtosecond laser for surface-enhanced Raman scattering," Optics Express, vol. 17, no. 24, p. 21581, Nov. 2009.
[2] S. N. Erkızan et al., "LIPSS for SERS: Metal Coated Direct laser written periodic nanostructures for Surface Enhanced Raman spectroscopy," Advanced Optical Materials, vol. 10, no. 22, Sep. 2022.

Control of fermentation process quality by infrared absorption spectroscopy

Lapins Adams[1,*], Chikvaidze Georgy[3], Gahbauer Florian[1], Klincare Ilze[1], Liepins Janis[2], Tamanis Maris[1]

[1] *Laser Centre, University of Latvia*

[2] *Institute of Solid State Physics, University of Latvia*

[3] *Institute of Microbiology and Biotechnology, University of Latvia*

[*] *E-mail:* adams.lapins@lu.lv

Fermentation processes harness the power of microorganisms to produce products such as fermented foods and drinks, acetic acid, and ethanol. Precise conditions are necessary for the process to proceed optimally, otherwise undesirable by-products can be produced, which ruin the batch and could also be polluting. Among the markers of sub-optimal fermentation conditions are volatile organics. Therefore, infra-red absorption spectroscopy could be a potential tool for on-line monitoring of fermentation processes. We have carried out a concept study of the potential of infrared spectroscopy for such on-line monitoring.

The yeast strain *Kluyveromyces marxianus* DSM 5422 was cultivated in a benchtop fermenter with synthetic dextrose as a medium. The temperature, air flow rate, dissolved oxygen, and stirring speed were carefully controlled. One batch was produced under optimal conditions, whereas another batch was produced under conditions that should produce chemical markers, namely pure ethanol. Gas from the fermentation was captured in a cuvette and absorption spectra were obtained with a Vertex 80v FTIR Fourier-Transform spectrometer (see Fig. 1). The upper sample curve (red) shows no traces of ethanol, indicating a successful fermentation. The lower sample shows traces of ethanol (see the arrows), which would indicate that the fermentation process is not proceeding optimally and requires intervention. We will present initial results and discuss possible applications to online monitoring of such processes in industry.

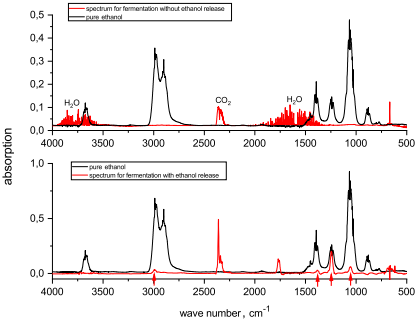

Figure 1: Infrared spectra of gases emitted during an optimal (upper plot) and suboptimal (bottom) fermentation process. Red curves – sample gas; black curves – ethanol reference spectrum.

Acknowlegments

We acknowledge support from Laserlab-Europe EU-H2020 Project No. 871124.

Molecular Gas References for Laser Wavelength Calibration in the 1530-1560 nm Range

Bilzens Alberts [1,*], Sedulis Arvids[1], Alnis Janis[1], Berzins Uldis[1]
[1] *University of Latvia, Institute of Atomic Physics and Spectroscopy*
[*] *E-mail:* alberts.bilzens@lu.lv

Our presentation looks into the utilization of acetylene (C2H2) and hydrogen cyanide (HCN) gases as molecular references for precise laser wavelength calibration within the 1530-1560 nm range. Leveraging distinct absorption features of these gases, we establish robust calibration standards. In addition to discussing experimental setups and calibration procedures, we explore simpler measurement techniques and ways for obtaining samples for acquiring these molecular references, including alternative approaches to measuring absorption spectra. The potential applications in telecommunications, spectroscopy, and metrology show their significance in advancing optical technology.

The saturated absorption spectroscopy method is also used, as it allows for studying the given molecular gas system with much higher resolution and accuracy than regular spectroscopy methods which use just single laser signal. [1,2]

These molecular references will be used in an upcoming project of measuring Sn negative ion energies and lifetimes of different states. The calibrated laser of 1535 nm wavelength will be used for exciting the negative ions so that their energies could be determined to a higher precision, and afterwards the lifetimes of the excited states could be measured. This experiment will provide results with a higher precision for gaining more information about the Sn- ion. [3,4]

Acknowledgments
This research is financed by the Fundamental and Applied Research Project (Nr. lzp-2023/1-0199): "The Laser Photodetachment Spectroscopy on Negative Ions", from Latvian Science Council.

References
[1] T. W. Hansch, I. S. Shahin, and A. L. Schawlow, "High-Resolution Saturation Spectroscopy of the Sodium D Lines with a Pulsed Tunable Dye Laser", Phys. Rev. Lett, 27, 708-710 (1971).
[2] Rajesh Thapa, Kevin Knabe, Mohammed Faheem, Ahmer Naweed, Oliver L. Weaver, and Kristan L. Corwin, "Saturated absorption spectroscopy of acetylene gas inside large-core photonic bandgap fiber," Opt. Lett. 31, 2489-2491 (2006)
[3] Moa K. Kristiansson, et al. High-precision electron affinity of oxygen. Nat Commun 13, 5906 (2022). https://doi.org/10.1038/s41467-022-33438-y
[4] U. Berzinsh, et al. Isotope shift in the electron affinity of chlorine. Phys. Rev. A 51, 231 (1995). https://doi.org/10.1103/PhysRevA.51.231

The effect of vascular resistance alterations on remote photoplethysmography signal

Obuhovskis Davids[1,*], Marcinkevics Zbignevs[1], Rubins Uldis[2], Lavrineca Ksenija[1], Grabovskis Andris[2]

[1] *Department of Human and Animal Physiology, Faculty of Biology, University of Latvia, Riga, Latvia;*

[2] *Biophotonics Laboratory, Institute of Atomic Physics and Spectroscopy, University of Latvia, Riga, Latvia.586;*

[*] *E-mail:* dobuhovskis@edu.riga.lv

Introduction. Vascular resistance is critical in cardiovascular physiology, influencing hemodynamics by regulating blood flow and systemic arterial pressure[1]. Its quantification is vital across various clinical and research areas. In cardiology, understanding vascular resistance is key to managing conditions like hypertension and heart failure and is essential in peripheral artery disease diagnosis and treatment. In critical care, it guides shock state management, while in sports science, it offers insights into cardiovascular adaptation to exercise. The present pilot study aimed to explore the impact of vascular resistance changes on remote photoplethysmography (PPG) signals.

Methods. Five healthy subjects aged 21 to 46 participated, with the study adhering to ethical standards and Local Ethical Committee approval. The protocol involved a bilateral leg thigh occlusion: a 3-minute rest, followed by sequential 3-minute suprasystolic occlusions on each thigh, and a 3-minute post-occlusion period. PPG signals were captured from the left hand using a custom PPG system (waveform characterizing parameter diastolic amplitude-Da), and systemic hemodynamics (mean arterial pressure-MAP, heart rate-HR, total vascular resistance –TPR) from the right hand by Finameter Midi hemodynamic monitor.

Results. During the resting stage, all subjects hemodynamic parameters remained within physiological ranges. At the onset of occlusion, there were transient changes in MAP, HR, and TPR, lasting for 20-30 seconds, characterized by a sharp decrease and increase in parameters. Following the stabilization period, occlusion of the left thigh led to an increase in MAP by 3-5%, TPR by 1.5-2%, and the PPG waveform parameter Da by 4-7%. A more pronounced increase in parameters was observed during the additional occlusion of the right thigh: MAP increased by 10-13%, TPR by 8-11%, and the PPG waveform parameter Da by 15-20%. A consistent decrease was observed during the post-occlusive hyperemic period: MAP decreased by 10-17%, TPR by 25-30%, and the PPG waveform parameter Da by 16-24%.

Conclusion. The study demonstrates that remote PPG waveform can reflect vascular resistance changes, suggesting its potential in diagnostics and exercise physiology, more research is needed to fully exploit this relationship.

Acknowledgments

This study was supported by Latvian Council of Science project FLPP-0326 (lzp-2022/1-0326)

References

[1] Trammel, J. E., & Sapra, A. (2024). Physiology, Systemic Vascular Resistance. StatPearls Publishing. https://www.ncbi.nlm.nih.gov/books/NBK556075

The reliability of automated sequential measurement of capillary refill time during systemic hemodynamic fluctuations

Zelca Una Undine[1,*], Balla Beate[1], Rubins Uldis[2], Marcinkevics Zbignevs[1], Grabovskis Andris[2]

[1] *Department of Human and Animal Physiology, Faculty of Biology, University of Latvia, Riga, Latvia;*

[2] *Biophotonics Laboratory, Institute of Atomic Physics and Spectroscopy, University of Latvia, Riga, Latvia.586;*

[*] *E-mail:* zelcaunaundine@gmail.com,

Introduction. Vascular Capillary Refill Time (CRT) stands as a crucial index in the medical field, offering a rapid, non-invasive measure for assessing micro circulation[1]. Its determination involves manually applying pressure to a digit, such as a nail bed or fingertip, and observing blanching, followed by timing the period for blood vessels to refill with oxygenated blood. Clinically CRT is essential in detecting shock and assessing treatment effectiveness, with a normal range below 2 seconds. Extended CRT may suggest poor circulation and health concerns, including dehydration. In pediatric care, a CRT over 3 seconds is particularly alarming, indicating serious illness and increased mortality risk. Despite the recognized importance of CRT in medical diagnostics, its manual measurement remains subjective, lacking measurement standardization.

Present pilot study aimed to evaluate the reliability of automated capillary refill time measurement device prototype during fluctuations of systemic hemodynamic parameters.

Methods. Occlusion protocol was utilized to manipulate systemic hemodynamic parameters, which might influence refill time. Protocol comprises 3 minutes resting period, 6 minutes occlusion of pneumatic cuff on the left and 3 min on the right thigh, with the following 3 minute post occlusion period. Central hemodynamic variables (arterial pressure-MAP, total peripheral resistance-TPR) were recorded in beat –per beat manner using Finameter Midi noninvasive monitor. Capillary refill time was measured at 15 sec intervals using a custom prototype with an optoelectronic system, applying and removing 1 kg force on a 0.8 cm^2 finger area. The signal was recorded at 525nm light, providing refill time (Tr).

Results and conclusion. During rest, subjects had normal hemodynamic parameters. At occlusion onset, MAP and TPR briefly fluctuated for 20-30 seconds. Post-stabilization, left thigh occlusion increased TPR by 1.5-2%, MAP by 3-5%, but Tr decreased by 10-15%. Additional right thigh occlusion caused a larger increase: TPR by 8-11%, MAP by 10-13%, but Tr decreased by 15-35%. In the post-occlusive hyperemic period, TPR and MAP steadily decreased by 25-30% and 10-17% respectively, while Tr increased by 10-15%. CRT changes were tied to these hemodynamic fluctuations

Conclusion, the automated sequential determination of CRT provides reliable measurements, hence it reflect changes in systemic hemodynamic parameters like arterial

pressure, suggesting its potential as a viable and more objective alternative to current manual techniques in the future.

Acknowledgments
This study was supported by Latvian Council of Science project FLPP-0326 (lzp-2022/1-0326)

References
[1] S. Fleming et al., "The Diagnostic Value of Capillary Refill Time for Detecting Serious Illness in Children," PLoS One, vol. 10, no. 9, e0138155, Sep. 2015.

Influence of various precursors on activated strontium aluminate synthesized by microwave-assisted hydrothermal method

Krizmane Katrina[1,*], Leimane Madara[1], Vitola Virginija[1], Einbergs Ernests[1], Zolotarjovs Aleksejs[1]

[1] *Institute of Solid State Physics, University of Latvia*

[*] *E-mail:* katrina.krizmane@cfi.lu.lv

Eu^{2+}, Dy^{3+} activated strontium aluminate has the properties of a long-lasting phosphor, with literature indicating an afterglow duration exceeding 10 hours. Typically, $SrAl_2O_4$: Eu^{2+}, Dy^{3+} is synthesized by solid-state route in relatively high temperatures under a reducing atmosphere. However, the microwave-assisted hydrothermal method has attracted attention due to homogeneous heating in the microwave process and small particle formation with narrow size distribution. To date, the literature does not describe how various precursors affect the morphology of the obtained samples and their luminescent properties.

In this work, various rare earth ion-activated strontium aluminate samples were synthesized using different precursors, such as KOH, LiOH, NaOH, HMTA, K_2CO_3, $(NH_4)_2CO_3$, and Na_2CO_3. These samples were prepared via the microwave-assisted hydrothermal synthesis route. The composition of crystalline phases ($SrAl_2O_4$, $Sr_3Al_2O_6$, $SrAl_4O_7$) was determined in the samples, as well as the morphology of the obtained samples was examined with the SEM method, and the luminescence emission spectra and luminescence quenching kinetics were examined. Luminescence at 500 - 520 nm, corresponding to the Eu^{2+} transition $4f^6 5d^1 \rightarrow 4f^7$, was observed in the obtained samples. Additionally, in certain samples, a peak at 353 nm suggested Eu^{2+} incorporation into the $Sr_3Al_2O_6$ structure. It was concluded how the use of different precursors influences the optical properties and morphological characteristics of $SrAl_2O_4$:Eu^{2+}, Dy^{3+}, and B^{3+}.

Acknowledgments

The financial support provided by Scientific Research LZP FLPP No. lzp-2023/1-0521 “Light activated 4D printed materials for vascular tissue engineering” is greatly acknowledged.

Evolution of ZnS:Cu nanoparticle morphology during microwave-assisted hydrothermal method

Dile Milena[1,*], Laganovska Katrina[1], Vanags Edgars [1], Smits Krisjanis [1], Vitola Virginija[1]

[1] *Institute of Solid State Physics, University of Latvia*

[*] *E-mail:* milena.dile@cfi.lu.lv

Doped ZnS materials exhibit excellent optical and electrical properties making them a superior material for photoluminescent and electroluminescent devices, solar panels, light-emitting diodes, laser diodes, and other device design and fabrication. The formation of specific ZnS particle morphology like nanoflowers is highly sensitive to reaction conditions. Therefore real-time monitoring of synthesis product properties may provide useful information about chemical reaction kinetics. Monitoring of the resulting nanoparticles in a conventional hydrothermal reaction is limited, however, specially designed equipment for microwave-assisted hydrothermal (MWHT) synthesis may enable in situ sampling procedure. Other advantages of MWHT such as fast reaction rates, uniform mixture heating, and more precise control over reaction conditions make this method very attractive. This study the possibility to perform sampling during MWHT synthesis of Cu-doped ZnS materials using sodium dodecyl sulfate was demonstrated. The obtained results substantiate formation of a cubic ZnS phase with crystallite size 3-5 nm. Moreover, formation and the subsequent dissolution of the ZnO hexagonal phase was observed. STEM figures elucidate that formation of ZnO is accompanied with formation and growth of flower-like ZnS structures. PL intensity of the resulting products with band positioned at 2,00 eV increases over time indicates transition between copper (II) ion energy levels.

Acknowledgments

Financial support provided by European Regional Development fund project Nr. 1.1.1.1/21/A/055 "Enhancing transparency and efficiency of scalable thin film electroluminescent protective panels using anti-reflective layers and advanced materials" realized at the Institute of Solid State Physics, University of Latvia is greatly acknowledged. Institute of Solid State Physics, University of Latvia as the Center of Excellence has received funding from the European Union's Horizon 2020 Framework Programme H2020-WIDESPREAD-01-2016-2017-TeamingPhase2 under grant agreement No.739508, project CAMART2.

References

[1] L. Zhang, L. Yang, Hydrothermal growth of zns microspheres and their temperature-dependent luminescence properties, Crystal Research and Technology (2008).

[2] A. Kuzmin, M. Dile, K. Laganovska, A. Zolotarjovs, Microwave-assisted synthesis and characterization of undoped and manganese doped zinc sulfide nanoparticles, Mater. Chem. Phys. (2022).

[3] A. L. Curcio, L. F. da Silva, M. I. B. Bernardi, E. Longo, A. Mesquita, Nanostructured ZnS:Cu phosphor: Correlation between photoluminescence properties and local structure, J. Lumin.(2019).

Improvement of fusional vergence performance during vision training

Jakovica Anastasija[1,*], Bisofa Anda[1], Eigusa Krista[1], Kosona Anastasija[1], Vercinska Emija[1], Krumina Gunta[1]

[1] *University of Latvia, Department of Optometry and Vision Science, Riga, Latvia*

[*] *E-mail:* anastasija.jakovica@lu.lv

Introduction. In today's world, the importance of eye care has increased significantly due to the growing number of people suffering from vision impairment - a trend influenced by various aspects of modern lifestyles. The ubiquity of digital devices has led to significant eye and vision disorders such as dry eye syndrome, visual discomfort, progressive myopia and an increase in the incidence of binocular vision disorders. These visual impairments are not only linked to prolonged time spent in front of large and small screens [1], [2] but also to a lack of active rest [3], which is essential for eye health, and to the increasing number of people with diabetes [4]. The functionality of our visual system goes beyond the structure of the eye and depends on the brain's ability to process visual stimuli [5]. Our study aimed to explore vision training approaches and their effectiveness.

Method. The computer games "Gnome" and "Arrow" employ the stereogram method utilizing random dots. Participants utilize anaglyph glasses to perceive distinct images for each eye. Their objective involves integrating these disparate images, represented as two squares, into a singular image through a fusional vergence process. During this integration, participants are tasked with discerning spatial shapes, whereby the spatial effect's disparity is modulated by altering the background or stimulus disparity. Subsequently, participants use keyboard arrows to manoeuvre the descending shape to its corresponding shape positioned at the bottom of the square. Following every sixth session, the participant's visual functions are tested.

Results. The following trends were observed when analysing the results: the improvement in convergent fusional vergence with training is significantly higher than the improvement in divergent fusional vergence; convergent vergence is faster, especially when small prisms are used, which promotes faster image fusion. In contrast, divergent fusion is also more difficult with small prisms and takes longer to fuse two images.

Conclusion. The results show that it is possible to train both convergent and divergent fusional vergence. Convergent fusional vergence improves more than divergent fusion.

References

[1] Blehm C. et al. Computer vision syndrome: a review. *Survey of Ophthalmology*, 50(3), 253-262, (2005).

[2] Rosenfield M. Computer vision syndrome: a review of ocular causes and potential treatments. *Ophthalmic and Physiological Optics*, 31, 502–515, (2011).

[3] Harrington S. et al. Visual factors associated with physical activity in schoolchildren. *Clinical and Experimental Optometry*, 106:6, 645-655, (2023).

[4] Ackland P. et al. World blindness and visual impairment: despite many successes, the problem is growing. *Community Eye Health*, 30, 71-73, (2017).

[5] Ciuffreda KJ. The scientific basis for and efficacy of optometric vision therapy in nonstrabismic accommodative and vergence disorders. *Optometry*, 73(12), 735-762, (2002).

Cataracts effects on colour vision

Truksa Renars[1], Bicevska Elize[1], Jansone-Langina Zane[1], Fomins Sergejs[2], Solomatins Andrejs[3]

[1] *Optometry and Vision Science Department, University of Latvia, Riga, Latvia*
[2] *Institute of Solid State Physics, University of Latvia, Riga, Latvia*
[3] *Dr. Solomatin Eye Rehabilitation and Vision Correction Centre*
[*] *E-mail:* rt08004@lu.lv

Individuals with cataracts experience a significantly greater absorption of light in the crystalline than the age-appropriate norm, resulting in a significant reduction in colour resolution and changes in colour perception. It is found that after cataract surgery, regardless of the age of the patients, the visual perception system demonstrates the ability to adapt to new lighting conditions.

Within the framework of the study, the effect of cataract surgery on colour resolution and changes in colour perception was evaluated using the FM100 hue test and the computerized colour vision test created by the authors. Within the framework of the study, sixteen people before cataract surgery and 5 people before and after cataract surgery were examined with the FM100 hue test and the computerized test, which provides the determination of the coordinates of the achromatic point.

When evaluating the results of the study participants, a statistically significant difference in performance was confirmed between individuals without cataracts and those scheduled for cataract surgery. When evaluating the performance of the study participants before and after cataract surgery, statistically significant differences in the FM100 hue test were found only for the GY-Y colour category.

The results of the study confirm that persons with cataracts have a statistically significantly higher number of errors in the FM100 hue test than the age-appropriate norm. The results of the study suggest that, despite the age of the study participants, their visual perception system demonstrates the ability to adapt to drastic changes in the spectral composition of lighting.

Colour vision in normal aging

Truksa Renars[1], Jansone-Langina Zane[1], Fomins Sergejs[2]
[1] *Optometry and Vision Science Department, University of Latvia, Riga, Latvia*
[2] *Institute of Solid State Physics, University of Latvia, Riga, Latvia*
[*] *E-mail:* reenaars@inbox.lv

As people get older, a gradual decrease in the light transmission of the crystalline lens is observed, which results in a significantly reduced colour resolution in the short wavelength part of the visible light spectrum. The analysis of the results of the FM100 hue test provides an opportunity to identify the part of the visible light spectrum in which individuals have a significantly reduced colour resolution. 130 persons aged between 20 and 70 years of age participated in the study. The colour vision of each individual was evaluated with colour vision tests CAD and FM100. As part of the study, a mathematical model was created to assess whether the increase in the number of errors in the short-wave portion of visible light can be explained by the increased light absorption in the crystalline lens. The results of the study confirm a statistically significant increase in the number of errors as the age of the study participants increases, as well as a statistically significant increase in the values of the chromatic sensitivity thresholds detected by the CAD test. The mathematical model created as part of the study correctly predicts a gradual increase in the number of errors in the FM100 hue test as the age of individuals increases. The results of the study suggest that the increase in light absorption in the crystalline lens explains the increase in the number of errors in the FM100 hue test.

WWW.DOCRIGA.LV

SPIE. STUDENT CHAPTER UNIVERSITY OF LATVIA

UNIVERSITY OF LATVIA

82nd International Scientific Conference of the University of Latvia 2024

UNIVERSITY OF LATVIA
INSTITUTE OF ATOMIC PHYSICS AND SPECTROSCOPY